

## TUMOUR MECHANOPATHOLOGY

## Cutting the stress out

Solid stress within tumours can be quantified by measuring their deformation after cutting or slicing or by taking a needle biopsy of them.

Daniele M. Gilkes and Denis Wirtz

The role of biomechanics in cancer cell biology has begun to draw widespread attention<sup>1–3</sup>. Tissue stiffening, which arises from intratumoural fibrosis resulting from abnormal extracellular-matrix deposition, remodelling and post-translational modifications to extracellular-matrix components<sup>4–6</sup>, is nowadays well recognized as a characteristic of many solid tumours. Stress within solid tissues is also a key biomechanical cue that cancer cells and their microenvironment can alter<sup>7,8</sup>; in fact, the external application of pressure contributes to the stimulation of important oncogenic signalling (such as the  $\beta$ -catenin pathway<sup>9</sup>). Yet the lack of methods to map solid stress within a tumour has precluded the study of how this biomechanical marker changes as a function of tumour progression. Now, writing in *Nature Biomedical Engineering*, Rakesh Jain and colleagues fill this gap by reporting three methods to quantify solid stress (and also the related elastic energy) in tumour tissue *ex vivo* and *in situ*<sup>10</sup>.

In one method, Jain and co-authors encapsulated freshly excised tumours formed in the brain, breast or pancreas of mice in 2% agarose, and then made a planar cut across the agarose-embedded tumour. The authors determined the magnitude and spatial distribution of solid stress within the tumour by using ultrasonography to map the three-dimensional deformation that occurs after the cut as the tumour mechanically relaxes (Fig. 1a). The authors observed that tumours from the pancreas and breast displayed compressive stress in the tumour's central region and tensile stress at the tumour periphery, whereas brain tumours experienced annular compressive stress towards their periphery, with maximum values ranging from 0.21 kPa (brain) to 7 kPa (pancreas). Interestingly, breast tumours depleted of collagen (achieved by using a collagenase treatment *ex vivo*) displayed a twofold reduction in stress compared with untreated breast tumours. Given that collagen architecture<sup>11</sup> is closely linked to tumour stiffness<sup>12</sup>, and that both properties are prognostic markers of breast

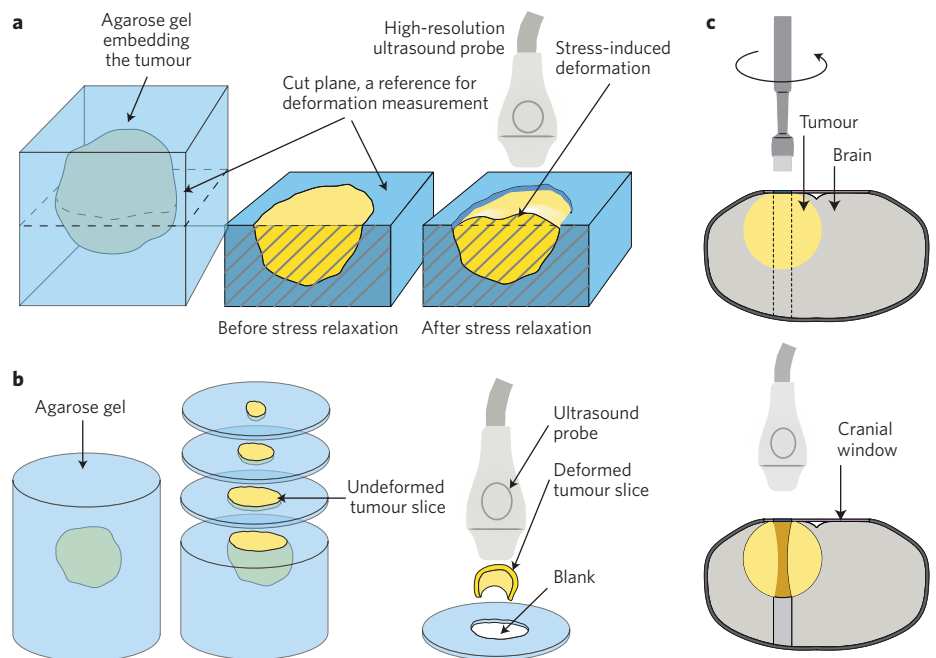


**Figure 1** | Three methods for measuring solid stress in *ex vivo* tumours<sup>10</sup>. **a**, In the planar-cut method, a freshly excised tumour is embedded in 2% agarose and then gelled in ice water. After planar excision and stress relaxation (the release of solid stress resulting from tumour deformation), an ultrasound probe can be used to map the deformation field of the relaxed tumour with respect to the reference plane defined by the cut. **b**, In the tissue-slice method, the tumour-encapsulating agarose gel is sliced into thin sections by a vibratome to measure via ultrasound the overall surface-area expansion with respect to the reference area of the tumour slice before slicing. The larger deformation of the sliced tissue, compared with that of the bisected tissue (planar-cut method in **a**), increases the sensitivity of the measurement. **c**, In the needle-biopsy method, the ultrasound probe measures changes in diameter along the cylindrical void left by the core needle after tissue relaxation. This method allows for *in situ* and *ex vivo* measurements. In all three methods, solid stress is calculated from the measurements via mathematical modelling. Figure adapted from ref. 10, Nature Publishing Group.

cancer<sup>13</sup>, it would be interesting to use this planar-cut method to measure solid stress in human tumours and correlate it with reported values for collagen architecture and stiffness<sup>11,12</sup>.

By using the planar-cut approach, Jain and co-authors also compared solid stress in primary tumours and metastases. Primary pancreatic tumours, formed by implanting pancreatic ductal adenocarcinoma cells into the pancreas of mice, exhibited larger stresses compared with size-matched liver

metastases formed from the same initiating cells. The opposite trend was observed in the case of colon cancer cells and size-matched liver metastases. Interestingly, stiffness (measured by an unconfined compression test in both primary and metastatic sites) was similar in both the pancreatic and colon cancer models. The authors concluded that stiffness and solid stress (and thus elastic energy) in tumour tissues are uncoupled. In other words, stiffer tumours do not always have higher elastic energy, and tumours

with high elastic energy are not necessarily stiffer. In view of this, it would be important to determine which measurement type — stiffness or solid stress — provides the most reliable biomechanical marker for tumour progression and for metastasis. Each biomarker may actually uncover unique mechanobiological insights about a tumour or its metastatic site. Indeed, Jain and co-authors' findings suggest that measurements of solid stress may provide clues about the influence of the tumour microenvironment (in particular, that of the metastatic site) on tumour biology that might not be uncovered by investigating tissue stiffness alone.

To investigate how solid stress accumulates during tumour growth, the authors used a slicing approach to determine solid stress in tumours ranging from 2 to 7 mm in diameter, derived from an adenocarcinoma model of breast cancer. After embedding the tumours in 2% agarose, they used a vibratome — an instrument that uses a vibrating razor blade to cut through tissue — to generate multiple slices of the agarose-encapsulated tissue thin enough (100–500 µm) to allow the slices to buckle and freely deform as solid stress is released as a result of the increase in exposed surface area (Fig. 1b). The agarose gel served as a template of the original tumour cross-section. The authors observed that the release of elastic energy after slicing was equal to the expansion in surface area, and that whereas small tumours did not show an increase in surface-area expansion, large tumours expanded by 30–40%. Yet stiffness measurements (by using atomic force microscopy-based indentation) did not show differences with tumour size, again suggesting that tissue stiffness and solid

stress are uncoupled. Given the sensitivity of the assay, it would be interesting to compare the stiffness of the liver of a healthy mouse with that of a tumour-bearing mouse prior to metastasis to the liver to determine whether the organ undergoes a change in elastic energy before the arrival of cancer cells or if cancer cells are required for the observed changes in tissue stiffness.

To take into account stress responses influenced by normal tissue surrounding *in vivo* tumours, Jain and co-authors used a core needle biopsy to quantify solid stress *in situ* by measuring, via ultrasonography, changes in the diameter of the cylindrical void left by the biopsy (Fig. 1c). They observed that solid stress determined *in situ* in U87-derived brain tumours surrounded by normal brain and cranium was higher than that of the tumours when the measurement was taken *ex vivo* after tumour removal. This suggests that normal tissue surrounding the tumour may play a vital role in influencing the biomechanical properties of the tumour tissue itself. Hence, using the needle-biopsy method, one could also determine the increase in solid stress in an organ by comparing the solid stress of normal brain tissue and of cancerous brain tissue *in situ*.

Therapies aimed at reducing mechanical stress within tumours with the goal of stabilizing blood vessels are currently being tested in clinical trials. These include losartan<sup>14</sup>, an angiotensin inhibitor, and PEGPH20 (ref. 15), a recombinant human hyaluronidase enzyme that temporarily degrades hyaluronan, an extracellular-matrix component. In view of this, it stands to reason that new methods are needed to monitor tissue mechanics as a diagnostic metric to predict the effectiveness of

treatments. Using agarose to embed tumours may be a practical hindrance for pathologists and surgeons, but modifying the current technique to overcome these challenges may lead to new diagnostic methods that could prove useful for the stratification of patients that respond favourably to treatments targeting the biomechanical properties of tumours. Also, future experiments that delineate the biological outcomes of increased stiffness compared with solid stress may lead to deeper insight into the processes of tumourigenesis and metastasis. □

Daniele M. Gilkes and Denis Wirtz are in the Department of Oncology, The Sidney Kimmel Comprehensive Cancer Center, The Johns Hopkins University School of Medicine, and the Department of Chemical and Biomolecular Engineering, Physical Sciences in Oncology Center, and Institute for Nanobiotechnology, The Johns Hopkins University, Baltimore, Maryland 21218, USA.  
e-mail: wirtz@jhu.edu

#### References

1. Wirtz, D., Konstantopoulos, K. & Searson, P. C. *Nat. Rev. Cancer* **11**, 512–522 (2011).
2. Goetz, J. G. *et al. Cell* **146**, 148–163 (2011).
3. Lopez, J. I., Mouw, J. K. & Weaver, V. M. *Oncogene* **27**, 6981–6993 (2008).
4. Gilkes, D. M., Semenza, G. L. & Wirtz, D. *Nat. Rev. Cancer* **14**, 430–439 (2014).
5. Paszek, M. J. *et al. Cancer Cell* **8**, 241–254 (2005).
6. Provenzano, P. P., Inman, D. R., Eliceiri, K. W. & Keely, P. J. *Oncogene* **28**, 4326–4343 (2009).
7. Helminger, G., Netti, P. A., Lichtenbeld, H. C., Melder, R. J. & Jain, R. K. *Nat. Biotechnol.* **15**, 778–783 (1997).
8. Stylianopoulos, T. *et al. Proc. Natl Acad. Sci. USA* **109**, 15101–15108 (2012).
9. Ou, G. & Weaver, V. M. *Bioessays* **37**, 1293–1297 (2015).
10. Nia, H. T. *et al. Nat. Biomed. Eng.* **1**, 0004 (2016).
11. Conklin, M. W. *et al. Am. J. Pathol.* **178**, 1221–1232 (2011).
12. Lu, P., Weaver, V. M. & Werb, Z. *J. Cell Biol.* **196**, 395–406 (2012).
13. Choi, W. J. *et al. Ultrasound Med. Biol.* **40**, 269–274 (2014).
14. Kumar, V. *et al. Transl. Oncol.* **9**, 431–437 (2016).
15. Provenzano, P. P. *et al. Cancer Cell* **21**, 418–429 (2012).